

Microrheology of Biopolymer-Membrane Complexes

E. Helfer,¹ S. Harlepp,¹ L. Bourdieu,^{1,*} J. Robert,¹ F. C. MacKintosh,² and D. Chatenay¹

¹Laboratoire de Dynamique des Fluides Complexes, U.M.R. C.N.R.S. 7506, Université Louis Pasteur, Strasbourg, France

²Department of Physics, University of Michigan, Ann Arbor, Michigan 48109-1120

(Received 7 December 1999)

We create tailored microstructures, consisting of complexes of lipid membranes with self-assembled biopolymer shells, to study the fundamental properties and interactions of these basic components of living cells. We measure the mechanical response of these artificial structures at the micrometer scale, using optical tweezers and single-particle tracking. These systems exhibit rich dynamics that illustrate the viscoelastic character of the quasi-two-dimensional biopolymer network. We present a theoretical model relating the rheological properties of these membranes to the observed dynamics.

PACS numbers: 87.19.Tt, 68.10.Et, 82.65.-i, 87.80.-y

Whereas the elasticity of fluid membranes has been studied extensively, less is known experimentally about viscoelastic, solid, or polymerized membranes because few examples of these have been found [1]. The presence of a finite shear modulus raises new dynamical properties with respect to those of fluid membranes, whose energy is characterized solely by bending [2]. We have created artificial, self-assembled complexes of lipid membranes and 2D-reticulated actin filaments that mimic cytoskeletal networks present in cells [3]. Both of these components have been widely studied in the past in isolation. In the case of actin, the viscoelasticity of actin filament solutions has been studied in detail: Because of its large persistence length ($L_p \sim 17 \mu\text{m}$) [4], the elastic and loss moduli have a frequency dependence ($G_{3D}' \sim G_{3D}'' \sim f^{0.75}$ for $f \gg 1 \text{ Hz}$) different from that of flexible polymers [5–7]. To study the dynamics of these composite membranes, we set up a microrheology experiment. We measure with high precision thermally excited position fluctuations of micrometer beads attached to them. For small deformations, we show how displacements perpendicular to the membrane plane (“out of plane”) are related to the membrane bending elasticity and those parallel (“in plane”) are linked to its in-plane shear viscoelasticity. Both in-plane and out-of-plane measurements show clear evidence of the viscoelastic nature of the composite membranes.

Our *in vitro* model consists of a thin shell of actin filaments polymerized and reticulated on the outside of giant unilamellar vesicles ($\sim 20 \mu\text{m}$ diameter) grown by electroformation [8]. They consist of a mixture of 95% of DOPC and 5% of DOPE-B which has a biotin group attached to its polar head [9]. Actin-coated vesicles are obtained by mixing the vesicles with biotinylated actin filaments (average length of $10 \mu\text{m}$) [10] in the presence of streptavidin. This creates stable biochemical bonds between filaments and lipids and cross-links between filaments themselves. The structure of the network is not precisely known [11], but the thin fluorescent contour of the vesicles observed in microscopy (see inset of Fig. 1) indicates that they are homogeneously coated with a dense actin shell. Moreover, the self-assembling of the actin network on the mem-

brane induces a decrease of its thermal undulations, as evidenced visually by the disappearance of the vesicle shape fluctuations.

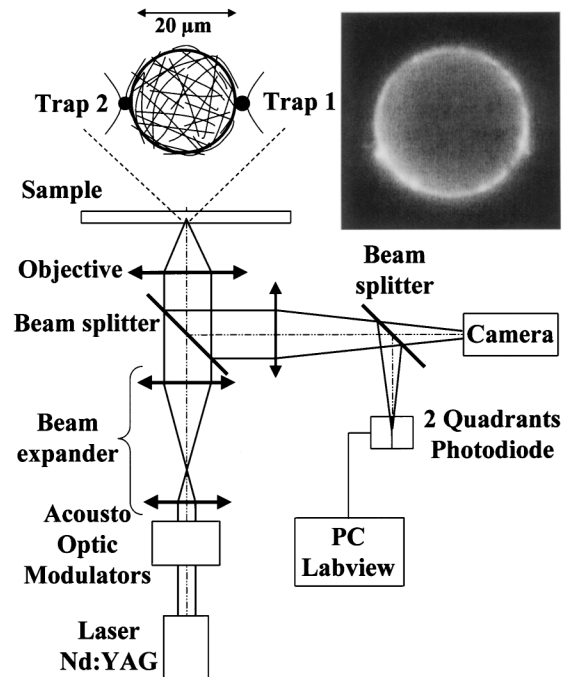


FIG. 1. Schematic of the experimental setup. An infrared laser (Topaz Nd:YAG 1064 nm, Spectra Physics) is focused with a high numerical aperture objective (Plan Neofluar 100 \times , NA 1.3, Zeiss). Two acousto-optic modulators (AA.DTS.XY-250, A&A Opto-Electronique) can deflect rapidly the laser beam to create two traps [11]. The infrared backscattered light is used to make an image of the bead on a two quadrants photodiode (S3096-02, Hamamatsu). The currents delivered by the quadrants are converted into voltages through $10 \text{ k}\Omega$ resistances. Their difference is amplified by a low-noise amplifier (SR-560, Stanford Research Systems) with a 30 kHz bandwidth and acquired with a Lab-PC1200 acquisition board at 60 kHz. The power spectrum of the position fluctuations of the probe beads is computed using a custom software written with LABVIEW. We show in the inset the picture of a fluorescent vesicle ($14 \mu\text{m}$ diameter) coated with actin filaments.

In order to quantify the effect of the actin network on the vesicle elasticity, we track the Brownian motion of streptavidin coated beads bound with optical tweezers to the composite membranes (i.e., to biotinylated actin monomers). Results are compared to those obtained with fluid vesicles, without the actin shell (the bead is attached to biotinylated lipids). The principle of the measurement is illustrated by the following simple example. For a trapped bead (radius R_b) in solution, the power spectrum of its position fluctuations is [12]

$$\langle x^2(f) \rangle = \frac{2\zeta k_B T}{4\pi^2 \zeta^2 f^2 + k^2}, \quad (1)$$

where $x(t)$ is the bead position in time, $x(f)$ is its Fourier transform, $\zeta = 6\pi\eta R_b$ is the drag coefficient on the bead in the fluid of viscosity η , and k is the trap stiffness. When the bead is attached to a vesicle, the power spectrum is modified due to the forces exerted by the membrane on the bead. The membrane energy consists of a sum of a bending term [2] (with modulus κ) and, in the case of actin-coated membranes, a term related to the in-plane viscoelasticity (2D complex modulus $G = G' + iG''$). In this case, the power spectrum depends on k , η , κ , and G . Therefore, changes in the spectrum before and after attachment to a vesicle are directly associated with the membrane mechanical properties.

The optical trapping experiment and the position detection setup are implemented on a home-built microscope (Fig. 1). The spectrum of the position fluctuations of the probe bead is obtained before its attachment to a vesicle. A Lorentzian fit to the data provides both the trap stiffness and the calibration factor [12]; above the trap corner frequency $f_c = k/2\pi\zeta$, a power law of exponent -2.00 ± 0.02 , consistent with Brownian motion, is fitted to the spectrum. Then the bead is bound to the membrane, and its spectrum is computed and compared to the previous one [13]. In practice, we use a trap stiffness as low as possible (10 to 50 Hz): Above f_c the spectrum does not depend on k but only on the membrane properties and on the solvent viscosity. The bead motion is measured in two directions, perpendicular to the membrane (out of plane) and parallel to the membrane (in plane): In-plane fluctuations will be related to membrane in-plane viscoelasticity, whereas out-of-plane fluctuations will be linked to the membrane bending elasticity.

The power laws given below are the best fits to the data between about 50 Hz (imposed by the low trap corner frequency) and 1 kHz in the case of fluid membranes [13] and 4 kHz in the case of actin-coated ones [14]. One to two decades in frequency correspond to two to four decades in the spectrum amplitude: this allows us to distinguish between close power law exponents.

On Fig. 2 are shown examples of power spectra obtained for the out-of-plane motion of 1.5 μm beads weakly

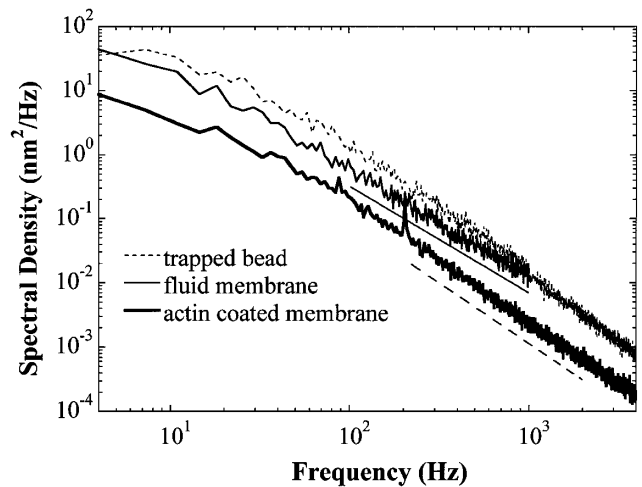


FIG. 2. Power spectra of the out-of-plane position fluctuations of 1.5 μm trapped beads: in solution, attached to a fluid membrane and attached to an actin-coated one. Above the trap corner frequency (~ 20 Hz in each case), power laws of exponent -2.01 ± 0.02 (trapped bead), -1.68 ± 0.03 (fluid membrane), and -1.88 ± 0.01 (actin-coated membrane) are best fits to these data. The curve for the fluid membrane shows the expected crossover to Brownian motion above about 1 kHz (note the overlap with the curve for an optical trap alone). The lines $f^{-1.68}$ (continuous) and $f^{-1.88}$ (dashed) are drawn as guides to the eye.

trapped ($k \sim 10^{-6}$ N/m) and attached either to a fluid or to an actin-coated membrane. For fluid membranes, the amplitude of the power spectrum (which is the same from one experiment to another) is lower than the one of a trapped bead alone. A power law with an exponent of -1.70 ± 0.05 best fits our data between 50 Hz and 1 kHz. The error bar is obtained from a statistical study of 12 curves measured with 4 different vesicles and 1 or 1.5 μm beads (this statistical error is indeed larger than the one calculated for each spectrum using a least squares method). For actin-coated membranes, an even smaller amplitude is observed. The amplitude drops from fluid to actin-coated vesicles by a factor of 3 ± 1 at 500 Hz, depending on the actin-coated vesicle. Moreover, a slightly but systematically different power law with an exponent of -1.85 ± 0.07 is measured (24 curves and 11 vesicles).

The out-of-plane position fluctuations of a point on the membrane are related, for small displacements, to its bending energy [2,15]: $E_b = (1/2)\kappa \int (\nabla^2 h)^2 ds$, where $h(r)$ is the membrane transverse position at the coordinate \mathbf{r} of a planar reference state. Using the equipartition theorem, the mean square amplitude of a mode \mathbf{q} is $\langle |h_q|^2 \rangle = k_B T / \kappa L^2 q^4$, where $h_q = \int h(r) e^{-iqr} d^2\mathbf{r}$ and L^2 is the membrane area; its relaxation frequency is $\omega_q = \kappa q^3 / 4\eta$ [16]. The time correlation of the height fluctuations being $\langle h_q(t) h_q(0) \rangle = \langle h_q^2 \rangle e^{-\omega_q t}$ [17], the Fourier transform leads to the out-of-plane power spectrum as a function of the frequency:

$$\begin{aligned} \langle \delta h^2(\omega) \rangle &= 2 \sum_q \langle h_q \rangle^2 \frac{\omega_q}{\omega^2 + \omega_q^2} \\ &= \frac{k_B T}{\kappa \pi} \int_0^{+\infty} \frac{dq}{q^3} \frac{\omega_q}{\omega^2 + \omega_q^2}. \end{aligned} \quad (2)$$

Note that upper and lower limits of integration depend on the bead size (radius R_b) and vesicle size (radius R_v), respectively. But the asymptotic result for large R_v and small R_b depends on κ and f as [17]

$$\langle \delta h^2(f) \rangle \propto \kappa^{-1/3} f^{-5/3}. \quad (3)$$

In the presence of the probe bead, this expression holds as long as the fluctuation wavelength, $\lambda = 2\pi/q$, is large compared with the bead size: Above a crossover frequency f_0 the power spectrum should be that of simple bead diffusion. Using the dispersion relation and the condition $\lambda \sim R_b$, one gets $f_0 \sim \kappa \pi^2 / \eta R_b^3$, which lies around a few kHz for a $1.5 \mu\text{m}$ bead attached to a fluid membrane [$\kappa \sim (10-20)k_B T$ [2,18]]. As indicated above, we observe a regime with a power law (-1.70) in agreement with the predicted one ($-5/3$). Moreover, with $6 \mu\text{m}$ beads, the power spectra for a trapped bead and for a bead bound to a fluid membrane ($f_0 \sim 30$ Hz) are the same, as predicted by the model (data not shown).

In the presence of the actin network, the reduced amplitude of the power spectrum results from an increase in κ . By comparing the amplitudes of the spectra of fluid and actin-coated vesicles ($\kappa^{-1/3}$ dependence), we infer a bending modulus of the composite membrane that is between $100k_B T$ and $1000k_B T$ at 500 Hz, depending on the vesicle. As mentioned above, we also measure a different power law exponent (-1.85 ± 0.07). This feature can be explained by a frequency dependence of the bending modulus [see Eq. (3)]. For an actin network of thickness h , we expect $\kappa \approx h^2 G'(f)$ [15]. From Eq. (3) and the measured exponent of -1.85 , our results are consistent with $\kappa \sim f^{0.55 \pm 0.21}$. This dependence in frequency reflects the viscoelastic character of the composite membrane.

If we consider now the in-plane fluctuations, dynamical regimes distinct from the out-of-plane motion are expected. In Fig. 3 are shown typical in-plane power spectra of a $1 \mu\text{m}$ bead attached to a fluid vesicle and to an actin-coated one and the fluctuation spectrum of a trapped bead. Within our experimental accuracy, the in-plane spectra for a bead attached to a fluid vesicle and for a trapped bead alone are identical for different bead sizes. This indicates that fluid membranes exert a negligible viscous drag on the bead with respect to that of the solution. In the case of the actin-coated membrane, the power spectrum of the in-plane fluctuations is shifted to smaller amplitudes and the power law exponent is -1.85 . The amplitude can vary by a factor of 3 depending on the vesicle, but the same exponent (-1.85 ± 0.07) is observed (18 curves, 8 vesicles, and 1 or $1.5 \mu\text{m}$ beads).

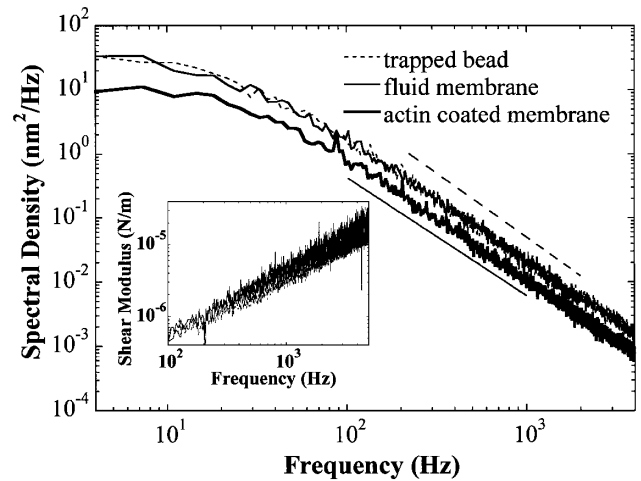


FIG. 3. Power spectra of the in-plane motion of $1 \mu\text{m}$ trapped beads: in solution, attached to a fluid membrane and attached to an actin-coated one. Above the trap corner frequency (~ 20 Hz) power laws of exponent -2.00 ± 0.02 (trapped bead), -1.99 ± 0.02 (fluid membrane), and -1.87 ± 0.02 (actin-coated membrane) are best fits to these data. The lines f^{-2} (dashed) and $f^{-1.87}$ (continuous) are drawn as guides to the eye. The inset shows the frequency dependence of the shear modulus: $G'(f)$ is deduced above the trap corner frequencies from the power spectra of in-plane position fluctuations obtained with $1 \mu\text{m}$ beads and three different vesicles.

The in-plane dynamics involves both shear viscoelasticity of the actin shell and the shear viscosity of the fluid. The power spectrum of the in-plane position fluctuations of a point on the membrane is computed as follows. We assume that the actin-coated membrane is characterized by a complex 2D modulus $G(f) = G'(f) + iG''(f)$. A force F in the membrane plane induces an in-plane displacement $u(f) \cong F/4\pi G(f)$. Using the fluctuation-dissipation theorem, one obtains [5]

$$\langle \delta u^2(f) \rangle \cong \frac{k_B T}{4\pi^2 f} \frac{G''(f)}{G'^2(f) + G''^2(f)}. \quad (4)$$

Assuming that the moduli G' and G'' scale with frequency [as is the case for bulk actin solutions [5-7]: $G_{3D}'(f) \sim G_{3D}''(f) \sim f^z$] and knowing that $G'' = G' \tan(\pi z/2)$ [19], the power spectrum of the in-plane fluctuations at high frequencies varies as

$$\langle \delta u^2(f) \rangle \cong \frac{k_B T}{4\pi^2 f G'(f)} \frac{\tan[(\pi/2)z]}{1 + \tan^2[(\pi/2)z]} \propto f^{-(1+z)}. \quad (5)$$

This expression holds as long as the viscous drag on the bead ($\zeta 2\pi f u$) is smaller than the elastic force due to the network [$4\pi G'(f)u$]. When the former dominates, a crossover to simple Brownian motion is again expected. The cutoff frequency f_1 is a solution of the equation obtained when the two forces are of the same magnitude:

$f_1 \sim G'(f_1)/3\pi\eta R_b$. By measuring the response of actin-coated membranes to a tangential deformation applied with a trapped bead (data not shown), the zero-frequency shear modulus G_0 is estimated to be about 0.5 to 5 $\mu\text{N/m}$. A lower estimate of f_1 is given by $G_0/3\pi\eta R_b \sim 200$ Hz for $R_b = 0.5$ μm . Only below this crossover are the fluctuations expected to provide a measure of the complex shear modulus $G(f)$.

In experiments performed with 1 and 1.5 μm diameter beads, a power law exponent of -1.85 ± 0.07 is measured. $G'(f)$ is directly calculated using Eq. (5) (inset of Fig. 3). At high frequencies, it appears that $G'(f)$ scales as $f^{0.85}$ ($z = 0.85 \pm 0.07$), providing also a self-consistent estimate of f_1 of about 10 kHz. There is a difference with respect to the exponent measured for κ (0.55 ± 0.21), although the observed exponents are not inconsistent with a common exponent of $z = 0.75$ (as expected, based on previous experiments [5,6] and theory [7] for bulk F-actin solutions). The difference may, however, be due to a relation between κ and G' more complicated than the one for a homogeneous plate of thickness h [$\kappa \approx h^2 G'(f)$ [15]].

Using micromechanical experiments we have characterized the elasticity of micrometer-sized, actin-coated vesicles. We have shown that the presence of an actin network significantly increases the bending stiffness of the membrane and demonstrates viscoelasticity. By detecting both in-plane and out-of-plane dynamics, we are able to characterize the shear and bending moduli of the membrane-polymer complex. We obtain power law dependence in frequency for the shear modulus [$G'(f) \sim f^{0.85 \pm 0.07}$] and for the bending modulus [$\kappa(f) \sim f^{0.55 \pm 0.21}$]. These exponents constitute a quantitative indication of the viscoelastic character of the actin shell, independent of the precise structure (e.g., concentration) of the network attached to the membrane.

This work was supported in part by Fondation pour la Recherche Médicale. We thank T. Duke and C. Marques for fruitful discussions. F.C.M. was supported in part by the CNRS, the NSF (DMR-9257544), and the Whitaker Foundation.

*To whom correspondence should be addressed.

- [1] *Statistical Mechanics of Membranes and Surfaces*, edited by D. Nelson, T. Piran, and S. Weinberg (World Scientific Publishing, Singapore, 1989).
 [2] W. Helfrich, *Z. Naturforsch.* **28c**, 693 (1973). For a review, including dynamics, see U. Seifert, *Adv. Phys.* **46**, 13 (1997).

- [3] B. Alberts *et al.*, *Molecular Biology of the Cell* (Garland Publishing, New York, 1994).
 [4] A. Ott *et al.*, *Phys. Rev. A* **48**, 1642 (1993).
 [5] F. Gittes *et al.*, *Phys. Rev. Lett.* **79**, 3286 (1997); B. Schnurr *et al.*, *Macromolecules* **30**, 7781 (1997).
 [6] A. Palmer *et al.*, *Biophys. J.* **76**, 1063 (1999); T. Gisler and D. A. Weitz, *Phys. Rev. Lett.* **82**, 1606 (1999).
 [7] D. C. Morse, *Phys. Rev. E* **58**, 1237 (1998); F. Gittes and F. C. MacKintosh, *Phys. Rev. E* **58**, 1241 (1998).
 [8] M. I. Angelova *et al.*, *Springer Proc. Phys.* **66**, 178 (1992).
 [9] 1,2-Dioleoyl-sn-Glycero-3-Phosphocholine and 1,2-Dioleoyl-sn-Glycero-3-Phosphoethanolamine-N-(CapBiotinyl) purchased from Avanti Polar Lipids.
 [10] Actin is purified from chicken breast muscle using a standard protocol. For information, see J. D. Pardee and J. A. Spudich, *Methods Cell Biol.* **24**, 271 (1982). A fraction, 15%, of the monomers are labeled with biotin-iodoacetamide (purchased from Molecular Probes). Actin is polymerized in a high salt polymerization buffer (50 mM KCl, 1 mM ATP, 0.2 mM CaCl_2 , 2 mM Tris-HCl, 2 mM MgCl_2) and stabilized and labeled with rhodamine-phalloidin (purchased from Molecular Probes).
 [11] Fluorescence microscopy shows a thin shell of actin filaments attached to the membrane (an upper limit of the thickness h is of the order of 0.1 to 1 μm). Inside the shell, individual fluorescently labeled filaments are distinguishable (the network mesh size is estimated to lie around 0.1 to 1 μm).
 [12] F. Gittes and C. F. Schmidt, *Methods Cell Biol.* **55**, 129 (1998).
 [13] The setup of optical tweezers allows us to create several traps by time sharing of the beam [see J. Molloy, *Methods Cell Biol.* **55**, 205 (1998)]. In the case of fluid membranes, we need indeed to hold a second bead at a point diametrically opposed to the imaged bead to avoid the displacement of the whole vesicle. Actin-coated vesicles weakly adhere to the coverslip, which prevents large-scale motion. The sharing of the beam limits the maximum frequency of acquisition at 1 kHz.
 [14] This second limit corresponds to an unexplained crossover to a steeper regime in the power spectrum of a trapped bead that limits the frequency range available well above the noise level [5].
 [15] L. Landau and E. Lifchitz, *Théorie de l'Elasticité* (Editions Mir, Moscou, 1974).
 [16] F. Brochard and J. F. Lennon, *J. Phys.* **36**, 1035 (1975).
 [17] A. G. Zilman and R. Granek, *Phys. Rev. Lett.* **77**, 4788 (1996); R. Granek, *J. Phys. II (France)* **7**, 1761 (1997).
 [18] E. A. Evans and W. Rawicz, *Phys. Rev. Lett.* **64**, 2094 (1990).
 [19] M. Doi and S. F. Edwards, *The Theory of Polymer Dynamics* (Clarendon Press, Oxford, 1986).